Droplet Routing in the Synthesis of Digital Microfluidic Biochips*

Fei Su, William Hwang and Krishnendu Chakrabarty
Department of Electrical & Computer Engineering
Duke University, Durham, NC 27708
E-mail: {*fs,wlh, krish*}*@ee.duke.edu*

Abstract

Recent advances in microfluidics are expected to lead to sensor systems for high-throughput biochemical analysis. CAD tools are needed to handle increased design complexity for such systems. Analogous to classical VLSI synthesis, a top-down design automation approach can shorten the design cycle and reduce human effort. We focus here on the droplet routing problem, which is a key issue in biochip physical design automation. We develop the first systematic droplet routing method that can be integrated with biochip synthesis. The proposed approach minimizes the number of cells used for droplet routing, while satisfying constraints imposed by throughput considerations and fluidic properties. A real-life biochemical application is used to evaluate the proposed method.

1. Introduction

Microfluidics is rapidly emerging as a key enabling technology for the design of sensor systems for medical, pharmaceutical and environmental monitoring applications [1]. These sensor systems rely on miniaturized devices that can manipulate fluids at nanoliter and microliter scales; such devices are referred to interchangeably in the literature as microfluidic biochips, lab-on-a-chip, and bioMEMS [1, 2].

The so-called *first generation* microfluidic biochips were based on continuous liquid flow through fabricated microchannels, and they were designed for simple biochemical analyses or assays [1]. Recently, a *second-generation* paradigm has emerged that manipulates liquids as discrete nanoliter droplets on a two-dimensional array of electrodes. Following the analogy of digital electronics, this technology is referred to as *digital microfluidics* [2]. Due to their inherent properties of dynamic reconfigurability and architectural scalability, digital biochips can be used as programmable "microfluidic processors".

Over the next few years, the digital microfluidic platform is expected to lead to sensor systems for massively parallel bioassays and analysis. As a result, system integration and design complexity will emerge as major challenges. Current full-custom design techniques are inadequate for digital microfluidic biochips that execute a set of concurrent sensing tasks and require a high degree of run-time flexibility. Thus, there is a pressing need for biochip-specific computer-aided-design (CAD) tools for automated design and prototyping.

While research on device-level physical modeling and simulation of single microfluidic components has gained momentum in recent years [3, 4], less attention has been devoted thus far to system-level design automation tools. In order to properly harness the potential offered by digital microfluidics, we need to deliver to biochip designers the same level of system-level CAD support that is now commonplace in the IC industry.

Analogous to classical VLSI synthesis, a top-down system-level design automation approach can be used to relieve biochip users from the burden of manual optimization of assays and time-consuming hardware design. We can divide the synthesis procedure for a digital microfluidic biochip into two major phases, i.e., architectural-level synthesis and physical design. A behavioral model for a set of bioassays is first obtained from their laboratory protocols. Architectural-level synthesis is then used to generate a macroscopic structure of the biochip; this is analogous to a structural RTL model in electronic CAD [5]. Next, physical design creates the final layout of the biochip, consisting of the placement of microfluidic modules such as mixers and storage units, the routes that droplets take between different modules, and other geometrical details [6].

In this paper, we focus on a key problem in biochip physical design, i.e., droplet routing between modules, and between modules and I/O ports (i.e., on-chip reservoirs). The dynamic reconfigurability inherent in digital microfluidics allows different droplet routes to share cells on the microfluidic array during different time intervals. In this sense, the routes in microfluidic biochips can be viewed as *virtual routes*, which makes droplet routing different from the classical wire VLSI routing problem. Here we develop the first systematic routing method for digital microfluidic biochips; our approach attempts to minimize the number of cells used for droplet routing, while satisfying constraints imposed by performance goals and fluidic properties.

The remainder of the paper is organized as follows. In Section 2, we present an overview of digital microfluidic biochips. Related prior work is next discussed in Section 3. Section 4 formulates the problem of droplet routing in the biochip synthesis flow. Detailed experimental validation of the fluidic constraint rules used in the proposed routing method is also presented in this section. Based on this problem formulation, a comprehensive routing methodology is proposed in Section 5. In Section 6, we use a real-life bioassay application as a case study to evaluate the proposed method. Finally, conclusions are drawn in Section 7.

2. Background: Digital Microfluidic Biochips

The basic cell of a digital microfluidic biochip consists of two parallel glass plates, as shown in Figure 1. The bottom plate contains a patterned array of individually controllable electrodes, and the top plate is coated with a continuous ground electrode. The droplets containing biochemical

* This research was supported in part by the National Science Foundation under grant number IIS-0312352.

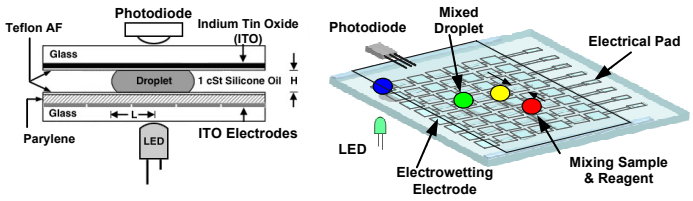

Figure 1: Schematics of a digital microfluidic biochip.

samples, and the filler medium, such as silicone oil, are sandwiched between the plates. By varying the electrical potential along a linear array of electrodes, droplets can be moved along this line of electrodes due to the principle of electrowetting [2, 3].

Using a two-dimensional array, many basic microfluidic operations for different bioassays can be performed, such as sample introduction (*dispense*), movement (*transport*), temporary preservation (*store*), sample dilution with buffer (*dilute*) and the mixing of different samples (*mix).* Note that these operations can be performed anywhere on the array, whereas in continuous-flow biochips they must operate in a specific micromixer or microchamber fixed on a substrate. This property is referred to as the dynamic reconfigurability of a digital microfluidic biochip. The configurations of the microfluidic array can be programmed into a microcontroller that controls the voltages of electrodes in the array.

As in digital circuit design, a module-based method can be applied to the design of digital microfluidic biochips. A microfluidic module library, analogous to a standard/custom cell library used in cell-based VLSI design, includes different microfluidic functional modules, such as mixers and storage units. We can map the microfluidic assay operations to available microfluidic modules, and then use architectural-level synthesis techniques to determine a schedule of sets of bioassays subject to precedence constraints imposed by the corresponding assay protocols [5]. The locations of the modules on the microfluidic array are then determined by the placement algorithms [6]. Therefore, these modules can be dynamically formed by activating the corresponding control electrodes during run-time. In this sense, the microfluidic modules can be viewed as virtual devices.

3. Related Prior Work

Wire routing is a well-studied problem in VLSI design. Due to the analogy between digital microfluidics and digital electronics, many classical VLSI routing techniques can be leveraged for the droplet routing problem [7, 8, 9]. However, there exist some important differences. For example, whereas electrical nets must not be short-circuited in VLSI routing, i.e., they cannot intersect each other, different droplet routes can be overlapped on some locations as long as they satisfy fluidic constraints. This is due to the property of *virtual nets* in digital microfluidic biochips, i.e., the droplet route is dynamically formed by sequentially activating the corresponding control electrodes. Consequentially, capacity constraints that result from fixed routing regions in VLSI design are not as important in droplet routing.

Recently reconfigurable devices, e.g., FPGAs and dynamic networks-on-chips (NoCs), have received much attention [10, 11, 12]. In order to overcome pin limitations of FPGA-based logic, some time-multiplexed routing methods such as Virtual Wires [13], have been proposed. Some packet routing algorithms are also proposed for NoCs [12]. By intelligently multiplexing each physical wire among multiple logical wires, such programmable routing is in some ways similar to the droplet routing problem. However, because of the differences in physical structure between FPGAs (NoCs) and digital microfluidic biochips, these time-multiplexed routing methods cannot be directly used for droplet routing. For example, unlike FPGAs that have well-defined roles of interconnect and logic blocks, there are no physical interconnects in digital microfluidic biochips. The same cells in the microfluidic array can be used for transporting droplets, as well as microfluidic operations such as mixing. Such features make the droplet routing problem different from FPGA/NoC routing. Moreover, instead of logical and electrical constraints, a different set of fluidic constraints need to be taken into account in droplet routing problem.

A channel routing problem for continuous-flow microfluidic biochips has been investigated in [14]. Since these biochips are fabricated in a single layer of glass, silicon or plastic, all microchannels must be routed in a planar fashion. Moreover, these microfabricated channels must not intersect. Thus, this routing problem is similar to the classical single-layer VLSI routing problem.

A problem related to droplet routing has been analyzed in [15], where the droplet path-planning problem for digital microfluidic biochips was modeled as a motion-planning problem with multiple moving robots. A prioritized A* search technique was presented. However, priority assignment, i.e., the order of droplet routing, becomes a crucial issue. It is hard to devise a general procedure that is suitable in all situations. In some extreme cases, low-priority droplet transport may take a long time; thus practical timing or throughput constraints are not considered in [15]. Another drawback in [15] is that only routes between two terminals are considered. However, many droplet routes connect multiple terminals when practical bioassays are applied to the digital microfluidic platform. Thus droplet pathways must be modeled as multi-pin nets.

A second approach for coordinating droplets in digital microfluidic biochips has been presented in [16]. By viewing the microfluidic array as a network, the authors reduced the droplet path-planning problem to a network flow problem. Since droplet motion is only limited to the fixed streets, this approach does not exploit some of the important benefits of digital microfluidics, e.g., dynamic reconfigurability.

4. Problem Formulation

4.1. Objective function

The main objective in routing is to find droplet routes with minimum lengths, where route length is measured by the number of cells in the path from the starting point to the destination. As discussed in [6], the microfluidic array consists of primary cells that are used in assay operations, and spare cells that can replace faulty primary cells for fault tolerance. Thus, for a microfluidic array of fixed size, minimum-length droplet routes lead to the minimization of

the total number of cells used in droplet routing, thus freeing up more spare cells for fault tolerance. This is especially important for safety-critical systems, an important application area for digital microfluidic biochips.

As in the case of electronic circuits, the fluidic ports on the boundary of microfluidic modules are referred to as *pins*, and we assume that pin assignment has been done in the placement phase. Similarly, we refer to the droplet routes between pins of different modules or on-chip reservoirs as *nets*. Thus, a fluidic route on which a single droplet is transported between two terminals can easily be modeled as a 2-pin net. We also need to move two droplets from different terminals to one common microfluidic module (e.g., mixer) for mixing. To allow droplet mixing simultaneously during their transport, which is preferable for efficient assay operations [2], we need to model such fluidic routes using 3-pin nets, instead of two individual 2-pin nets.

4.2. Fluidic constraints

During droplet routing, a minimum spacing between droplets must be maintained to prevent accidental mixing, except for the case when droplet merging is desired (e.g., in 3-pin nets). We view the microfluidic modules placed on the array as obstacles in droplet routing. In order to avoid conflicts between droplet routes and assay operations, a segregation region is added to wrap around the functional region of microfluidic modules. In this way, droplet routing can easily be isolated from active microfluidic modules.

For multiple droplet routes that may intersect or overlap with each other, fluidic constraint rules must be introduced to avoid undesirable behavior. Without loss of generality, we refer to two given droplets as D_i and D_j. First, to avoid mixing, we assume that their initial locations at time slot t are not directly adjacent or diagonally adjacent to each other. Let us represent the microfluidic array by two-dimensional coordinates (X, Y), and let $X_i(t)$ and $Y_i(t)$ denote the location of D_i at time t. We must ensure that either $|X_i(t) - X_j(t)| \geq 2$ or $|Y_i(t) - Y_j(t)| \geq 2$ for these two droplets. To select the admissible locations of the droplets at the next time slot t+1, fluidic constraint rules need to be satisfied as follows.

Rule #1: $|X_i(t+1) - X_j(t+1)| \geq 2$ or $|Y_i(t+1) - Y_j(t+1)| \geq 2$, i.e., their new locations are not adjacent to each other.

Rule #2: $|X_i(t+1) - X_j(t)| \geq 2$ or $|Y_i(t+1) - Y_j(t)| \geq 2$, i.e., the activated cell for droplet D_i cannot be adjacent to D_j. Otherwise, there is more than one activated neighboring cell for D_j, which may leads to errant fluidic operation.

Rule #3: $|X_i(t) - X_j(t+1)| \geq 2$ or $|Y_i(t) - Y_j(t+1)| \geq 2$.

Note that Rule #1 can be considered as the static fluidic constraint, whereas Rule #2 and Rule #3 are dynamic fluidic constraints.

We verified these fluidic constraint rules through a set of laboratory experiments. A simple digital microfluidic array was used as the platform for all experiments; electrodes 1 through 8 of this chip are labeled in Figure 2(a). The experimental setup is also shown in Figure 2(b).

The placements of droplets are shown in Figure 2(a) to illustrate minimum spacing requirement for static droplets. To demonstrate Rule #1 as shown in Figure 3(a), we forced

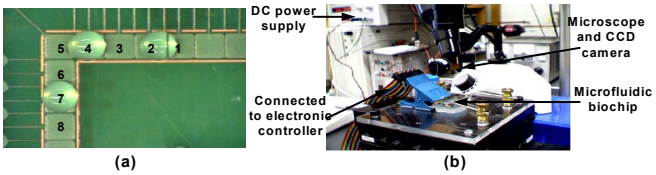

Figure 2: (a) A part of a digital microfluidic biochip for experiments; (b) Experimental setup.

droplets D_i and D_j to move by activating electrodes 2 and 3, and deactivating electrodes 1 and 4, simultaneously. Since the new locations of these two droplets, i.e., electrode 2 and 3, were adjacent to each other, they were in contact with each others' surfaces, as shown in Figure 3(b). To attain minimum surface energy, the two droplets merged into one droplet, which was centered equally over electrodes 2 and 3; see Figure 3(c). Obviously, the violation of Rule #1 leads to an unintended mixing of different droplets.

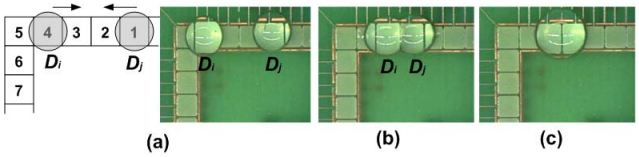

Figure 3: (a) Experimental verification of Rule #1: droplets begin on electrodes 1 and 4; (b) Electrodes 2 and 3 are activated, and 1 and 4 deactivated; (c) Merged droplet.

We next investigated the consequences of violating dynamic fluidic constraint rules, i.e., Rule #2 or Rule #3. As shown in Figure 4(a), two droplets D_i and D_j were placed on electrodes 4 and 7 initially. Then, to move D_i and D_j rightward and upward, respectively, electrodes 3 and 6 were actuated simultaneously. Unfortunately, Rule #3 was violated due to two activated neighboring cells for D_i (i.e., it is directly adjacent to electrode 3 and also diagonally adjacent to electrode 6). We observed that droplet D_j moved rapidly to electrode 6, while droplet D_i showed very little movement towards electrode 3, as Figure 4(b). Then they contacted each other, thus leading to the mixing of these two droplets, as shown in Figure 4(c).

The purpose of the above experiments was to demonstrate that adherence to Rule #1 is not sufficient to prevent merging. Both Rule #2 and Rule #3 must also be satisfied during droplet routing. Moreover, these fluidic constraint rules are not only used for rule checking, but they can also provide guidelines to modify droplet motion (e.g., force some droplets to remain stationary in a time-slot) to avoid constraint violation if necessary; the details of such a strategy are discussed in Section 5.3.

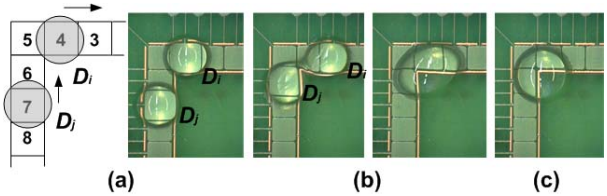

Figure 4: (a) Experimental verification of Rule #3: droplets begin on electrodes 4 and 7; (b) Electrodes 3 and 6 are activated, and 4 and 7 deactivated; (c) Merged droplet.

4.3. Timing constraints

Another important constraint in droplet routing is given by an upper limit on droplet transportation time. This constraint arises from a critical assumption made in the architectural-level synthesis of digital microfluidic biochips. It is assumed in [5] that since droplet movement on a microfluidic array is very fast compared to assay operations (e.g., mixing, dilution and optical detection), we can ignore the droplet routing time for scheduling assay operations. This assumption has been validated by laboratory experiments for simple assays. For example, it has been reported that mixing in a 2×4-array mixer takes about 10 seconds, whereas it takes only 10 ms for a droplet to move across one cell during its route (with 100Hz clock frequency) [17].

To ensure that the above assumption is valid for complex sets of concurrent assays, we need to ensure that the delay for each droplet route does not exceed some maximum value, e.g., 10% of a time-slot used in scheduling. Otherwise, the schedule obtained from the synthesis procedure is no longer valid. This timing constraint is analogous to the interconnect delay constraints in VLSI routing that require each wire net (or critical path) to meet its timing budget. Note that since a droplet may be held at a location in some time slots during its route, the delay for each droplet route is not identical to the route length. The delay for a droplet route therefore consists of the transport time as well as the idle time.

4.4. Problem decomposition

Since digital microfluidic biochips can exploit the dynamic reconfigurability of the microfluidic array during run-time, a series of 2-D placement configurations in different time spans, instead of one single 2-D placement in classical VLSI design, are obtained in the module placement phase [6]. In this way, we can decompose droplet routing into a series of sub-problems. In each sub-problem, the nets to be routed from the target module to the source module are determined first. Only the microfluidic modules that are active during this time interval are considered as obstacles in droplet routing. Next we attempt to find suitable routes for these nets. These sub-problems are addressed sequentially to obtain a complete solution for droplet routing.

5. Routing Method

This section presents the proposed droplet routing method. The quality of the solution obtained by this method is independent of the routing order of nets. The inputs to the algorithm are a list of nets to be routed in each sub-problem as well as constraints imposed by the designer.

The droplet routing algorithm consists of two basic stages. The first stage generates M alternative routes for each net, where M can be fine-tuned through experiments (e.g., we use $2 < M < 10$ in our work). The algorithm attempts to find the shortest routes for each net (2-pin net or 3-pin net). In addition, the obtained routes also need to pass the timing delay constraint check (TDCC) in this stage. Those that violate the timing constraint are pruned from the set of alternative routes. Note that if all the shortest routes for some net do not satisfy the timing constraint, placement refinement is required to increase the corresponding routability.

The second stage of the routing algorithm first randomly selects a single route from the alternatives for each net. The set of randomly-selected routes for a given net list then go through the fluidic constraint rule check (FCRC). If necessary, some modifications are made to the routes to ensure that all fluidic constraints are satisfied. The delay for the corresponding net is updated, and then TDCC is performed again. The objective function for this set of routes is also obtained by calculating the number of cells used in routing. Through an appropriate number of random selection runs, a set of routes with the minimum cost function, subject to both timing and fluidic constraints, is finally selected to be the output of the routing algorithm. If no suitable solution for droplet routing is found, routability-oriented placement refinement is invoked again. Advantages of the routing methodology described above include the avoidance of the net-routing-order dependence problem, and the use of dynamic reconfigurability. Some key details of the algorithm are as follows.

5.1. Phase I: *M*-shortest routes

In this phase, M alternative routes for each net are generated. We modify the Lee algorithm, a popular technique used in grid routing [8, 9], for the droplet routing problem in digital microfluidic biochips.

5.1.1. Two-pin nets. The shortest route problem for 2-pin nets is equivalent to the single-pair shortest path problem. An advantage of the Lee algorithm is that it is guaranteed to find the shortest path between two pins, which can be included among the M alternatives. We further modify the Lee algorithm to find M shortest paths for each net. Note that these M alternative routes may include the next shortest paths, the lengths of which are longer than the shortest one.

5.1.2. Three-pin nets. We use 3-pin nets to model the routes along which two droplets are transported towards a microfluidic module (e.g., a mixer); the droplets can mix together during their transportation. The shortest-route problem for such nets is equivalent to the Steiner Minimum Tree (SMT) problem [8]. Since SMT is known to be NP-hard, a heuristic approach is needed for this problem. We can also modify the Lee algorithm to address this problem.

5.2. Phase II: random selection

In the second phase of the algorithm, a single route from the M_i alternatives for each net i is selected, where $i \in \{1, 2, \ldots N\}$ and N is the number of nets. Note that $M_i \leq M$ since some routes that violate the timing constraint have already been eliminated. A random selection approach is then used to select i_k for each net i, where i_k represents the k-th alternative route for net i, and $k \in \{1, 2, \ldots, M_i\}$. A desirable feature of this random method is that it avoids the net-routing order dependence problem.

To evaluate the set of selected routes, we model the cost function as the total number of cells used in routing. It is represented by $C = \sum_{i=1}^{m \times n} X_i$, where the binary variable X_i is 1 if cell i in an $m \times n$ array is used in routing; otherwise, it is 0.

Constraint checking also needs to be performed for each set of selected routes. If it fails FCRC (including droplet

motion modification discussed in Section 5.3) or TDCC, we assign a large penalty value *Pt* to this set of routes. Otherwise, we set *Pt* = 0 for those that satisfy all constraints. After an adequate number of random selection runs, we select the set of routes with the minimum cost value *C* and *Pt* = 0 as the output of the routing algorithm.

5.3. FCRC and droplet motion modification

We note that in the first stage of the algorithm, *M* alternative routes for each net are obtained irrespective of the existence of other nets. However, since different net routes may share the same cells or they may be close to each other, we need to ensure that they do not violate the fluidic constraints stated in Section 4.2.

Assume that two droplet routes (i.e., P_i and P_j) have been obtained using the modified Lee algorithm. To adhere to fluidic constraint rules, we need to check these two droplets D_i and D_j in each time slot. Interestingly, even if a rule violation is found, we can still modify droplet motion (i.e., force a droplet to stay in the current cell instead of moving) to override the violation; see Table 1. If the modification fails (as in last the row of Table 1), the corresponding routing paths are deemed to be infeasible. We can further extend the modification to the case of more than two droplet pathways.

Table 1: Modification rules

Rule#1	Rule#2	Rule#3	Modification
Pass	Pass	Pass	Not required
Pass	Pass	Fail	D_j stays
Pass	Fail	Pass	D_i stays
Pass	Fail	Fail	N/A*
Fail	Pass	Pass	Droplet with the smaller $DL(P)$ stays
Fail	Pass	Fail	D_j stays
Fail	Fail	Pass	D_i stays
Fail	Fail	Fail	Fail

*N/A denotes that this case does not exist.

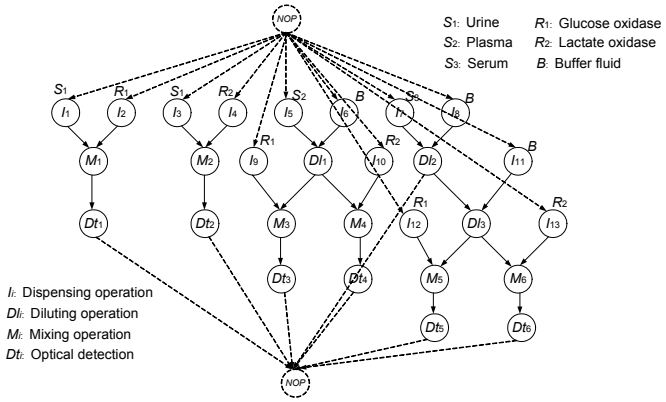

Figure 5: Sequencing graph model of assay example.

6. Experimental Evaluation

In this section, we evaluate the proposed droplet routing method by using it to design a biochip applied for a set of real-life bioassays, namely multiplexed *in-vitro* diagnostics on human physiological fluids.

As a typical example of multiplexed and concurrent assays, three types of human physiological fluids — urine, serum and plasma — are sampled and dispensed into the digital microfluidic biochip, and glucose and lactate measurements are performed for each type of physiological

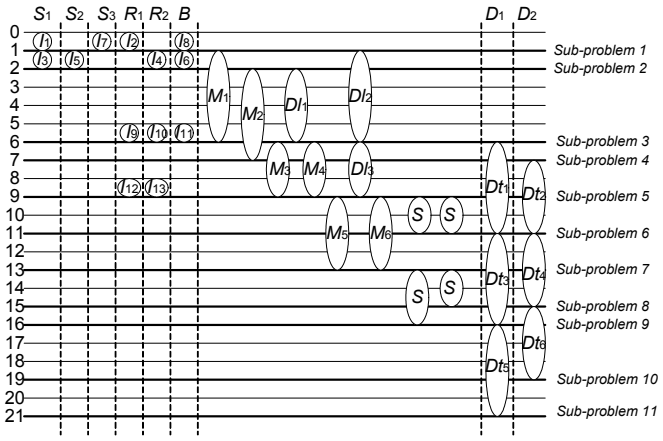

Figure 6: Schedule obtained via architectural-level synthesis.

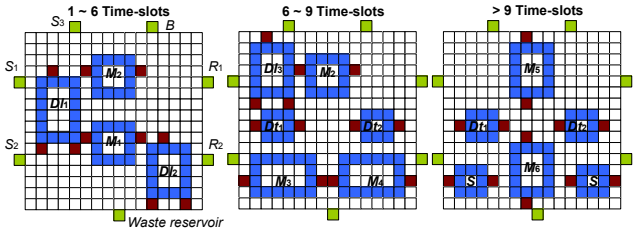

Figure 7: Module placement.

fluid. The assay protocol, based on Trinder's reaction [18], can be modeled by a sequencing graph, as shown in Figure 5.

We assume that an optimal schedule for assay operations as well as module usage have been obtained via architectural-level synthesis (e.g., through the modified list-scheduling algorithm [5]), as shown in Figure 6. Note that one time unit in this schedule is set to 2 seconds. Moreover, assume that a module placement on a 16×16 microfluidic array has also been given *a priori*, as shown in Figure 7.

To find suitable droplet routes for this biochip, we first use the method described in Section 4.4 to decompose the routing problem into eleven sub-problems, as highlighted in Figure 6. We address these sub-problems serially by attempting to find the set of droplet routes that use the minimum number of cells, subject to both the timing and fluidic constraints. Here we set the maximum delay constraint to 10% of one time unit in the schedule, i.e., 0.2 second. We also assume that the electrodes are controlled with a 100Hz clock frequency in the droplet route. Therefore, one time slot used in routing can be set to 10 ms, and the timing constraint *Td* is equal to 20 time-slots.

Here we use Sub-problem 3 to illustrate the two-stage routing method proposed in Section 5. As shown in Figure 8(a), there are three 2-pin nets and two 3-pin nets to be routed. Since the microfluidic module M_2 is active during this time interval, it is considered as an obstacle for routing. First, *M*-shortest routes for each net (*M* = 4 here) are obtained using the modified Lee algorithm. Unfortunately, all shortest paths between the dilutors DL_2 and DL_3 (i.e., Route 3) violate the timing delay constraint, i.e., $L(P)$ = 27 (in cells) > *Td* = 20 (time-slots). Thus, placement refinement is required to address this problem. One refinement example is shown in Figure 8(b). Note that this refined placement does not change other metrics (e.g., area) in placement, but it significantly

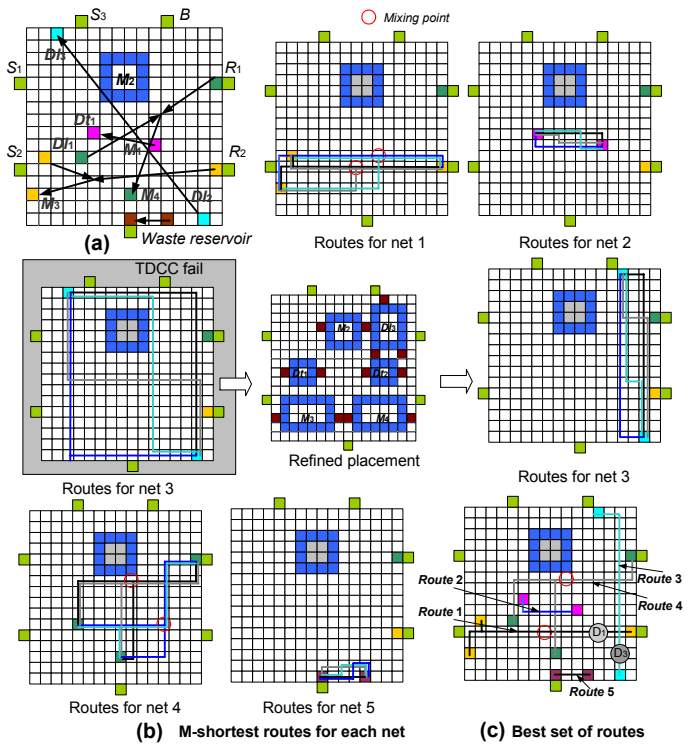

Figure 8: (a) Sub-problem 3; (b) M-shortest routes; (c) Selected set of routes.

eases the routing between DL_1 and DL_2. In the second stage of the routing algorithm, random selection is then performed to choose a single route from the four alternatives for each net. Also, TDCC, DCRC and modification are carried out for each set of route selection. Their cost values are also calculated, where Pt = 10000 if constraints are violated. The desirable solution with C = 57 and Pt = 0 is finally obtained, i.e., in total, there are 57 cells used in routing, and all routes satisfy timing delay constraint and fluidic constraint, as shown in Figure 8(c). Note that for droplets D_1 and D_3 in route 1 and 3 respectively, fluidic constraint rule #3 might be violated if they both move to the next cells at time slot 3. However, based on the modification rules on Table 1, we can force D_3 to stay in the current location at time slot 3, thereby overriding the constraint violation. The delay for route 3 is also updated to 18 time-slots by adding one time slot for the idle droplet.

In a similar manner, the routing results for all sub-problems can be easily obtained. (The details are not shown here due to lack of space.) This evaluation example shows that the proposed routing method can be easily used for the physical design of digital microfluidic biochips.

7. Conclusion

In this paper, we have presented a systematic routing method for digital microfluidic biochips. We first formulated the droplet routing problem, where the total number of cells used for routing serves as the objective criterion. Important constraints imposed by performance goals and fluidic properties have also been incorporated. A detailed experimental validation has been carried out for the fluidic constraint rules. Based on this problem formulation, a two-stage routing method has been proposed; this method is independent of the routing order of nets. We have also exploited the features of dynamic reconfigurability and independent controllability of electrodes to modify droplet pathways to override potential violation of fluidic constraints. The real-life example of a set of multiplexed bioassays has been used to evaluate the effectiveness of the proposed method. This method will next be integrated with architectural-level synthesis and module placement to form a comprehensive synthesis tool for digital microfluidic biochips. Therefore, the proposed biochip synthesis method is expected to facilitate the automated design of mixed-technology sensor systems for the emerging commodity market.

8. References

[1] E. Verpoorte and N. F. De Rooij, "Microfluidics meets MEMS", *Proc. IEEE*, vol. 91, pp. 930-953, 2003.

[2] V. Srinivasan et al., "An integrated digital microfluidic lab-on-a-chip for clinical diagnostics on human physiological fluids," *Lab on a Chip*, vol. 4, pp. 310-315, 2004.

[3] J. Zeng and T. Korsmeyer, "Principles of droplet electrohydrodynamics for lab-on-a-chip", *Lab on a Chip*, vol. 4, pp. 265-277, 2004.

[4] T. Korsmeyer et al., "Design tools for bioMEMS", *Proc. DAC*, pp. 622-627, 2004.

[5] F. Su and K. Chakrabarty, "Architectural-level synthesis of digital microfluidics-based biochips", *Proc. ICCAD*, pp. 223-228, 2004.

[6] F. Su and K. Chakrabarty, "Design of fault-tolerant and dynamically-reconfigurable microfluidic biochips", *Proc. DATE Conf.*, pp. 1202-1207, 2005.

[7] N. Sherwani, *Algorithms for VLSI Physical Design Automation*, Kluwer Academic Publishers, MA 1995.

[8] S. Sait and H. Youssef, *VLSI Physical Design Automation: Theory and Practice*, IEEE Press, NY, 1995.

[9] C. Sechen, *VLSI Placement and Global Routing Using Simulated Annealing*, Kluwer Academic Publishers, Boston, MA, 1988.

[10] R. Fung et al., "Simultaneous short-path and long-path timing optimization for FPGAs", *Proc. ICCAD*, pp. 838-845, 2004.

[11] L. McMurchie and C. Ebeling, "PathFinder: A negotiation-based performance-driven router for FPGAs", *Proc. ACM Symp. FPGAs*, pp. 111-117, 1995.

[12] M. Majer et al., "Packet routing in dynamically changing networks on chips", *Proc. Parallel and Distributed Processing Symp.*, pp. 154b-154b, 2005

[13] J. Babb et al., "Virtual wires: overcoming pin limitations on FPGA-based logic emulators", *Proc. IEEE Workshop on FPGA for Custom Computing Machines*, pp. 142-151, 1993.

[14] A. J. Pfeiffer et al., "Simultaneous design and placement of multiplexed chemical processing systems on microchip", *Proc. ICCAD*, pp. 229-236, 2004.

[15] K. F. Böhringer, "Towards optimal strategies for moving droplets in digital microfluidic systems", *Proc. IEEE Int. Conf. Robotics and Automation*, pp. 1468-1474, 2004.

[16] E. Griffith and S. Akella, "Coordinating multiple droplets in planar array digital microfluidics systems", *Workshop on the Algorithmic Foundations of Robotics*, 2004.

[17] P. Paik et al., "Rapid droplet mixers for digital microfluidic systems", *Lab on a Chip*, vol. 3, pp. 253-259, 2003.

[18] P. Trinder, "Determination of glucose in blood using glucose oxidase with an alternative oxygen acceptor", *Annals of Clinical Biochemistry*, vol. 6, pp. 24-27, 1969.